

Time-dependent variational approach to solve multi-dimensional time-dependent Schrödinger equation

Mingrui He(何明睿), Zhe Wang(王哲), Lufeng Yao(姚陆锋), and Yang Li(李洋)
Citation: Chin. Phys. B, 2023, 32 (**12**): 124206. DOI: 10.1088/1674-1056/acef03
Journal homepage: http://cpb.iphy.ac.cn; http://iopscience.iop.org/cpb

What follows is a list of articles you may be interested in

Role of quantum paths in generation of attosecond pulses

M R Sami and A Shahbaz†
Chin. Phys. B, 2020, 29 (**10**): 104207. DOI: 10.1088/1674-1056/ab9deb

Atomic even-harmonic generation due to symmetry-breaking effects induced by spatially inhomogeneous field

Yue Guo(郭月), Aihua Liu(刘爱华), Jun Wang(王俊), Xueshen Liu(刘学深)
Chin. Phys. B, 2019, 28 (**9**): 094212. DOI: 10.1088/1674-1056/ab37fa

Resolving multi-orbital effects on high harmonic generation from aligned N_2 molecules in linearly and elliptically polarized intense laser fields

Hong-Jing Liang(梁红静), Xin Fan(范鑫), Shuang Feng(冯爽), Li-Yu Shan(单立宇), Qing-Hua Gao(高庆华), Bo Yan(闫博), Ri Ma(马日), Hai-Feng Xu(徐海峰), Da-Jun Ding(丁大军)
Chin. Phys. B, 2019, 28 (**9**): 094211. DOI: 10.1088/1674-1056/ab3440

Femtosecond enhancement cavity with kilowatt average power

Jin Zhang(张津), Lin-Qiang Hua(华林强), Shao-Gang Yu(余少刚), Zhong Chen(陈忠), Xiao-Jun Liu(柳晓军)
Chin. Phys. B, 2019, 28 (**4**): 044206. DOI: 10.1088/1674-1056/28/4/044206

A tunable XUV monochromatic light source based on the time preserving grating selection of high-order harmonic generation

Yong Niu(牛永), Hongjing Liang(梁红静), Yi Liu(刘燚), Fangyuan Liu(刘方圆), Ri Ma(马日), Dajun Ding(丁大军)
Chin. Phys. B, 2017, 26 (**7**): 074222. DOI: 10.1088/1674-1056/26/7/074222

Time-dependent variational approach to solve multi-dimensional time-dependent Schrödinger equation

Mingrui He(何明睿)[1,†], Zhe Wang(王哲)[1], Lufeng Yao(姚陆锋)[1], and Yang Li(李洋)[2,‡]

[1] *Department of Basic Courses, Naval University of Engineering, Wuhan* 430033, *China*
[2] *Key Laboratory for Laser Plasmas (Ministry of Education) and School of Physics and Astronomy, Shanghai Jiao Tong University, Shanghai* 200240, *China*

(Received 26 April 2023; revised manuscript received 3 August 2023; accepted manuscript online 11 August 2023)

We present an efficient approach to solve multi-dimensional time-dependent Schrödinger equation (TDSE) in an intense laser field. In this approach, each spatial degree of freedom is treated as a distinguishable quasi-particle. The non-separable Coulomb potential is regarded as a two-body operator between different quasi-particles. The time-dependent variational principle is used to derive the equations of motion. Then the high-order multi-dimensional problem is broken down into several lower-order coupled equations, which can be efficiently solved. As a demonstration, we apply this method to solve the two-dimensional TDSE. The accuracy is tested by comparing the direct solutions of TDSE using several examples such as the strong-field ionization and the high harmonic generation. The results show that the present method is much more computationally efficient than the conventional one without sacrificing accuracy. The present method can be straightforwardly extended to three-dimensional problems. Our study provides a flexible method to investigate the laser-atom interaction in the nonperturbative regime.

Keywords: time-dependent variational approach, above-threshold ionization, high harmonic generation

PACS: 42.65.Ky, 42.65.Re, 32.80.Fb **DOI:** 10.1088/1674-1056/acef03

1. Introduction

The rapid development of laser technology brings powerful ultrashort intense light sources into laboratories.[1–3] The frequency domain of the modern laser covers a broad range from mid-infrared to the x-ray regime, while the intensity of the laser pulses is routinely achieved over 10^{16} W/cm^2. Atoms, molecules, and condensed matter interacting with the intense light sources exhibit various nonlinear phenomena, including above-threshold ionization (ATI),[4–6] high-order harmonic generation (HHG),[7–11] and nonsequential double ionization.[12,13] All these phenomena are not accessible through perturbation theory.

In the non-relativistic regime, numerically solving the time-dependent Schrödinger equation (TDSE) is the most rigorous nonperturbative method to simulate the intense laser-atom interactions, which in principle gives the most faithful reproduction of the concerned physical scenarios. However, as the computational resources required by solving TDSE grow exponentially with respect to the number of degrees of freedom, most discussions of full-dimensional systems are restricted to the single-active-electron (SAE) approximations.[14–16] Even within SAE, accurate solutions under extreme conditions are still challenging. They demand enormous computer resources for two- and three-dimensional models of atoms and molecules. Nowadays, efficient methods to solve TDSE are still under active development using different bases under different given physical conditions.[17–19]

The curse of dimensionality is more severe when SAE fails, if, for example, doubly excited states are important. A formal consistent way is to treat all electrons as active indistinguishable particles. Directly solving TDSE beyond simple multielectron species, such as He and H_2, is extremely difficult, due to exponential increase in computational cost. For example, when simulating full dimensional He on $L^2(\mathbb{R}^6)$ using a basis $\{e_1, e_2, \ldots, e_n\} \subset L^2(\mathbb{R})$, one needs to discretize, store, and apply the Hamiltonian H in this basis $H_{i_1 \ldots i_d j_1 \ldots j_d} = \langle e_{i_1} \otimes \ldots e_{i_d} | H | e_{j_1} \otimes \ldots e_{j_d} \rangle$. The tensor products $H_{i_1 \ldots i_d j_1 \ldots j_d}$ consists of n^{12} complex numbers, thus applying it requires n^{12} complex mutiplecations. However, to represent a physical situation to a satisfying accuracy, the discretization must be chosen high enough, i.e., n must be chosen to be large enough, which is limited by the available computational resources, especially for high-dimensional problems. To subjugate this difficulty, various theoretical methods, including the time-dependent density-functional theory (TDDFT) and the multiconfiguration time-dependent Hartree–Fock (MCTDHF) method have been proposed, which provide efficient resorts for quantum mechanics to treat multi-electron systems as *ab initio* as possible.[20–22] In the MCTDHF method, the total wavefunction of the multi-electron system is expressed as a superposition of the chosen number of time-dependent spin-orbitals prepared for each electron. It provides a compact and computationally less demanding description of the multi-electron atoms and molecules interacting with the in-

†Corresponding author. E-mail: hmr_emma@163.com
‡Corresponding author. E-mail: liyang22@sjtu.edu.cn

© 2023 Chinese Physical Society and IOP Publishing Ltd

tense light sources. The mathematical idea is to discretize a state in the configuration space of each electron. The electron–electron correlation, i.e., the interaction between each configuration space is approximated by low-rank approximation. An improved description of the electron correlation is achieved by adding more configurations in the singular value decompositions.

In this paper, inspired by the methodology of MCTDHF method for multielectron problems and math behind, we formulate an efficient method to solve multi-dimensional TDSE within single-electron approximation. Using two-dimensional (2D) TDSE as an example, we treat each spatial degree of freedom as a distinguishable quasi-particle. Then the 2D total electronic wavefunction is expressed as a linear combination of a direct product of one-dimensional (1D) wavefunctions with different expansion coefficients. Both the expansion coefficients and the 1D wavefunctions are simultaneously propagated in time based on the time-dependent variational principle,[21,23,24] which provides an adequate representation of the temporal evolution of the total wavefunction with appreciably less computational demand. We implement this approach to numerically simulate the strong-field ionization of the argon atoms induced by the linearly polarized laser pulse and circularly polarized laser pulse. With the increasing number of decomposing 1D wavefunctions, the obtained photoelectron momentum distributions (PEMDs) show increasingly better agreement with these simulated by numerically solving the TDSE directly. Moreover, we investigate the high harmonic generation (HHG) from a 1D non-Born–Oppenheimer hydrogen molecular ion. The obtained spectrum is in good agreement with the TDSE calculation. This provides an accurate and efficient method to simulate the laser-atom interaction within extreme electromagnetic conditions, which generally demands large computer power.

2. Numerical methods

2.1. Argon atom

We first consider the strong-field ionization of 2D model argon atom exposed to a strong laser field. The 2D-TDSE reads [atomic units (a.u.) are used throughout unless stated otherwise]

$$\mathrm{i}\frac{\partial}{\partial t}\psi(x,y,t) = H(x,y,t)\psi(x,y,t). \tag{1}$$

In length gauge, the Hamiltonian $H(x,y,t)$ is given by

$$H(x,y,t) = -\frac{1}{2}\frac{\partial^2}{\partial x^2} - \frac{1}{2}\frac{\partial^2}{\partial y^2} + V(x,y) + xE_x(t) + yE_y(t), \tag{2}$$

where $E_x(t)$ and $E_y(t)$ denote the orthogonal components of the laser electric field along x and y directions, respectively, and $V(x,y)$ is the soft Coulomb potential of argon atom,

$$V(x,y) = -\frac{1}{\sqrt{x^2+y^2+\varepsilon}}. \tag{3}$$

The soft-core parameter ε is set to be 0.39 to correctly reproduce the ground-state energy of the argon atom. Equation (2) is separable except for the soft Coulomb potential. In our time-dependent variational treatment, each spatial degree of freedom is regarded as a quasi-particle. It represents that we treat the two dimensions as independent degrees of freedom, while these two dimensions are not really independent because of the potential function. Therefrom, we separate the total Hamiltonian according to their spatial components as

$$H(x,t) = -\frac{1}{2}\frac{\partial^2}{\partial x^2} + xE_x(t), \tag{4}$$

$$H(y,t) = -\frac{1}{2}\frac{\partial^2}{\partial y^2} + yE_y(t), \tag{5}$$

together with the soft Coulomb potential (3) being the particle-particle interaction term.

Analogy to the MCTDHF method, we rewrite the total 2D wavefunction as a superposition of 1D wavefunction products

$$\psi(x,y,t) = \sum_{ij}^{n} c_{ij}(t)\chi_i(x,t)\phi_j(y,t). \tag{6}$$

We call $\chi(x,t)$ and $\phi(y,t)$ the 1D orbitals of x-particle and y-particle, respectively, and $c_{ij}(t)$ being the expansion coefficients. We would like to mention that, similar to performing eigenvalue decomposition on the square matrix, only when n equals the grid number of $\psi(x,y,t)$, the sum of the products of 1D wavefunction can produce exact 2D wavefunction $\psi(x,y,t)$. Here $\chi(x,t)$ and $\phi(y,t)$ are simulated by imaginary-time propagation, and orthonormalization is imposed on these 1D orbitals

$$\langle\chi_\mu|\chi_\nu\rangle = \delta_{\mu\nu}, \tag{7}$$

$$\langle\phi_\lambda|\phi_\gamma\rangle = \delta_{\lambda\gamma}. \tag{8}$$

With these assumptions at hand, we can derive the equations of motion for the 1D orbitals $\chi(x,t)$ and $\phi(y,t)$ as well as the expansion coefficients $c_{ij}(t)$ based on the time-dependent variational principle.[21,23] The results read

$$\begin{aligned}\mathrm{i}\frac{\partial}{\partial t}C_{ij}(t) = &\sum_{i'}\langle\chi_i|H(x,t)|\chi_{i'}\rangle C_{i'j}(t)\\ &+\sum_{j'}\langle\phi_j|H(y,t)|\phi_{j'}\rangle C_{ij'}(t)\\ &+\sum_{i',j'}\langle\chi_i\phi_j|V(x,y)|\chi_{i'}\phi_{j'}\rangle C_{i'j'}(t),\end{aligned} \tag{9}$$

$$\begin{aligned}\mathrm{i}\frac{\partial}{\partial t}\chi_i(x,t) = &\hat{Q}^{(x)}\{H(x,t)\chi_i(x,t)\\ &+\sum_{p,q}(\rho_x^{-1})_i^p\sum_{\mu,\nu}(\rho_{xy})_{p\mu}^{q\nu}(\hat{W}_{xy})_\nu^\mu\chi_q(x,t)\},\end{aligned} \tag{10}$$

$$\begin{aligned}\mathrm{i}\frac{\partial}{\partial t}\phi_i(y,t) = &\hat{Q}^{(y)}\{H(y,t)\phi_i(y,t)\\ &+\sum_{\mu,\nu}(\rho_y^{-1})_i^\mu\sum_{p,q}(\rho_{xy})_{\mu p}^{\nu q}(\hat{W}_{yx})_q^p\phi_\nu(y,t)\},\end{aligned} \tag{11}$$

where the operators $\hat{Q}^{(x)} = 1 - \sum_{\rm p} |\chi_{\rm p}\rangle\langle\chi_{\rm p}|$ and $\hat{Q}^{(y)} = 1 - \sum_{\mu} |\psi_{\mu}\rangle\langle\psi_{\mu}|$ are projectors onto the orthogonal complement of the occupied orbital space, which guarantee the orthonormality of orbitals during time propagation; ρ_x, ρ_y, and ρ_{xy} are the one-body and two-body reduced density matrices, respectively; $(\hat{W}_{xy})^{\mu}_{\nu}$ and $(\hat{W}_{yx})^{p}_{q}$ are mean-field potentials, given by

$$(\hat{W}_{xy})^{\mu}_{\nu}(x) = \int {\rm d}y \psi^*_{\mu}(y,t) V(x,y) \psi_{\nu}(y,t), \tag{12}$$

$$(\hat{W}_{yx})^{p}_{q}(y) = \int {\rm d}x \chi^*_{p}(x,t) V(x,y) \psi_{q}(x,t). \tag{13}$$

The fourth-order Runge–Kutta method is employed to numerically propagate the equations of motion. The initial wavefunction is prepared by imaginary-time propagation.[25] To obtain the PEMD, the total 2D wavefunction is split into two parts at the end of every time step by an absorbing function,[26,27] and the "ionized part" is first transformed into momentum space and then propagated under the Volkov Hamiltonian analytically to the end of the pulse.[26]

2.2. Hydrogen molecular ion

The second example is HHG from H_2^+ molecular ion subject to a linearly polarized laser field. The motions of the nuclei and electron are restricted in the polarization direction of the laser field. Then the Hamiltonian $H(z,R,t)$ can be modeled by

$$\begin{aligned} H(z,R,t) = &-\frac{1}{2\mu_{\rm e}}\frac{\partial^2}{\partial z^2} - \frac{1}{M}\frac{\partial^2}{\partial R^2} \\ &+ \frac{1}{\sqrt{R^2+\varepsilon_{\rm nn}}} - \frac{1}{\sqrt{(z-R/2)^2+\varepsilon_{\rm ne}}} \\ &- \frac{1}{\sqrt{(z+R/2)^2+\varepsilon_{\rm ne}}} - q_{\rm eff} z E_z(t), \end{aligned} \tag{14}$$

where z and R are the electronic coordinate as measured from the nuclear center of mass and the internuclear distance, respectively. The soft-core parameter $\varepsilon_{\rm nn}$ and $\varepsilon_{\rm ne}$ are set to be 1.0 and 0.03, respectively. The electronic reduced mass is given by $\mu_{\rm e} = 2M/(2M+1)$ with M being the proton mass. The effective charge is $q_{\rm eff} = (2M+2)/(2M+1)$. Similar to Eq. (2), we can decompose Eq. (14) into a set of single-particle Hamiltonians and the particle interaction term. The total wavefunction $\psi(z,R,t)$ is expanded accordingly. Then the equations of motion can be derived. Details are omitted here. HHG spectra are computed as the squared modulus of the Fourier-transformed electric dipole acceleration. In order to reduce the background level of the HHG spectra, the dipole acceleration is multiplied by a Hanning window function before the Fourier transform.

3. Results and discussion

We first consider the strong-field ionization of the argon atom subject to a linearly polarized few-cycle laser pulse with the wavelength of 1200 nm, the peak intensity of 2×10^{14} W/cm^2 and the pulse duration of $8T$ with T being the optical cycle period of the laser pulse. The electric field $\boldsymbol{E}(t)$ of the laser pulse is defined as

$$\boldsymbol{E}(t) = E_0 \sin^2(\pi t/T_{\rm p}) \cos(\omega t) \boldsymbol{e}_x, \quad 0 \le t \le N_0 T. \tag{15}$$

Here $\omega = 2\pi/T$ is the angular frequency. $N_0 = 8$ is the total number of the laser optical cycles. $E_0 = 0.0755$ is the amplitude of the electric field corresponding to the peak laser intensity of 2×10^{14} W/cm^2. With this intensity, the Keldysh parameter[28] $\gamma < 1$, i.e., in the tunneling regime. Here $\gamma = [I_{\rm p}/(2U_{\rm p})]^{1/2}$, with $U_{\rm p} = E_0^2/(4\omega^2)$ being the ponderomotive potential.

We employ two treatments to solve the 2D-TDSE: (1) The approximation method with the 2D electron wavefunction $\Psi(x,y,t)$ given by Eq. (6), using n 1D wavefunctions for both x and y directions. Figures 1(a)–1(e) present the obtained PEMD for different numbers n. (2) Numerically exact solution of the TDSE with split-operator spectral method[29] by discretizing 2D electron wavefunction in Cartesian grid ranges from -819 a.u. to 819 a.u. for both directions with the grid size of $\Delta x = \Delta y = 0.4$ a.u. The obtained PEMD is shown in Fig. 1(f), which works as a reference.

For small n, like $n = 1$, the calculated PEMD is not credible, and the interference structures cannot be identified in the spectrum. With increasing n, the PEMD simulated by the approximation method shows increasingly better agreement with the reference result in Fig. 1(f). When $n = 30$, the obtained PEMD (as shown in Fig. 1(e)) has no obvious difference with the reference result. By performing eigenvalue decomposition on the potential function $V(x,y)$, we obtain a simple criterion for selecting suitable n. For Ar atom, as n increases, the diagonal elements of the feature matrix rapidly decrease. Set the threshold 10^{-10} and $n = 30$.

In order to compare the numerical efficiency of the present method with the commonly used 2D representation of the wave function on grid, we first analyze the required memory size. Denoting the number of grid points along each direction by m, the required memory size for the expansion of Eq. (6) can be expressed as $2mn + n^2$ and that for the the conventional method as m^2. Typically, the condition $n \ll m$ is satisfied. Thus the required memory size for the 2D electron wavefunction in the present method is much smaller than that in the conventional method for achieving a good agreement. However, due to the 2D potential function $V(x,y)$ used in the temporal propagation, the memory size cannot be reduced in a further step. Moreover, thanks to the small size of the wavefunction, one can expect that the computational efficiency can be significantly improved. Numerical propagation of Eqs. (9)–(11) is much faster. The only price to pay is that Eqs. (10) and (11) are nonlinear, time step smaller than that in the common method should be adopted in order to have a stable propagation. Nevertheless, the computation time is 30% of the common method.

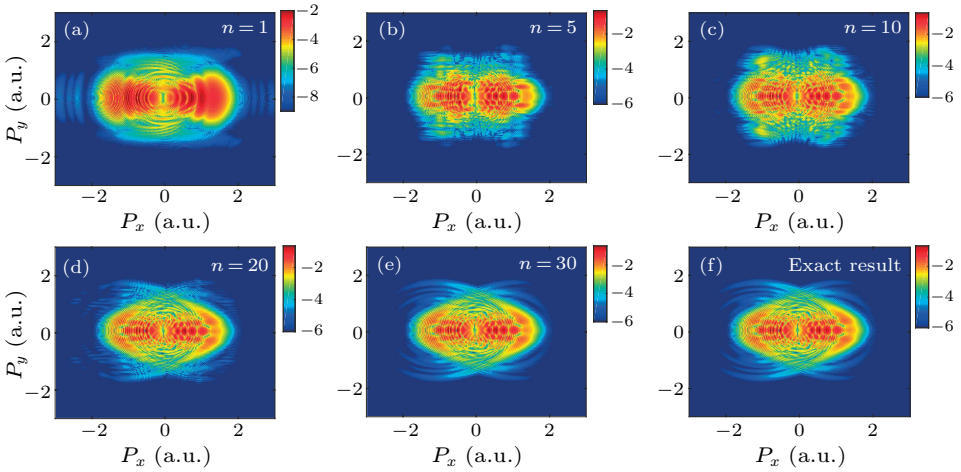


Fig. 1. The photoelectron momentum distribution (PEMD) of Ar atoms induced by the linearly polarized laser pulse, simulated by the approximation method [(a)–(e)] and the precise split-operator spectral method (f). The number n of the one-dimensional wavefunctions in the approximation method is (a) 1, (b) 5, (c) 10, (d) 20, and (e) 30. The wavelength of the laser pulse is 1200 nm and the intensity is 2×10^{14} W/cm^2. The pulse duration is 8 optical cycles. The color scale is logarithmic.

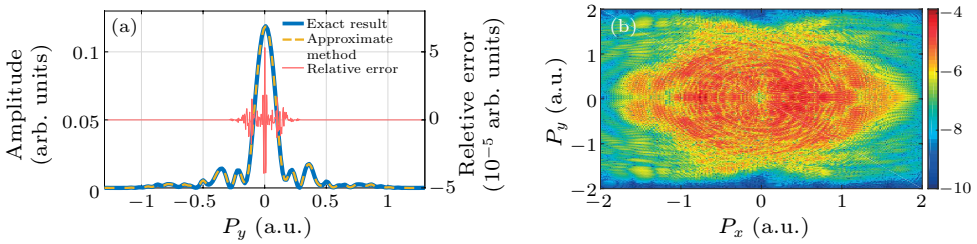


Fig. 2. (a) Left longitudinal coordinate: The transverse momentum distribution of the PEMD at the cut $p_x = U_p$ extracted from Fig. 1(e) (orange dashed curve) and Fig. 1(f) (blue curve). Right longitudinal coordinate: the relative error of the two curves (red curve). (b) The difference plot with logarithmic color scale.

Evident interference structures can be identified in Fig. 1(e). The nearly horizontal fork-like interference fringes are the strong-field photoelectron holography.[30] In previous studies, both the inherent structural information and the ultrafast electronic dynamical information can be retrieved from the phase of the interference fringes,[5,31,32] which requires our approximation method to provide correct interference fringe locations as carried out with the traditional TDSE solving method (including the split-operator spectral method). To make an intuitive comparison, we cut slices from Figs. 1(e) and 1(f) at $p_x = U_p$, respectively. The corresponding transverse momentum distributions are shown in Fig. 2(a), where the approximate result (orange dashed curve) almost exactly coincides with the reference result (blue curve). The relative error between these two curves, as shown by the red curve in Figs. 2(a), is in the order of 10^{-4} and below. Furthermore, a differential approach is used to compare the overall difference between Figs. 1(e) and 1(f). The difference plot is defined as $\mathrm{DP}(p_x,p_y) = |D_a(P_x,P_y) - D_{ref}(P_x,P_y)|$, where $D_a(P_x,P_y)$ and $D_{ref}(P_x,P_y)$ are the photoelectron distribution corresponding to the approximation method with $n = 30$ and the reference result, respectively. As shown in Fig. 2(b), the amplitude of $\mathrm{DP}(p_x,p_y)$ has been as low as 10^{-4} and the interference fringes in the PEMD have barely any location shift.

Besides the one-dimensional linearly polarized laser pulse, we investigate the tunneling ionization of argon atoms induced by a circularly polarized laser pulse. The laser parameters of this circularly polarized laser pulse, including the wavelength, peak intensity, and pulse duration are the same as the linearly polarized laser pulse. Here, the electric field $\boldsymbol{E}(t)$ of this laser pulse is defined as

$$\boldsymbol{E}(t) = \frac{\sqrt{2}}{2}E_0 \sin^2(\pi t/T_p)[\cos(\omega t)\boldsymbol{e}_x + \sin(\omega t)\boldsymbol{e}_y], \quad 0 \le t \le N_0 T. \tag{16}$$

Similarly, we employ both the approximation method and the split-operator spectral method to solve the 2D TDSE. For the approximation method, the number n of the one-dimensional wavefunctions used in Eq. (6) increases from 1 to 30, corresponding to PEMDs presented in Figs. 3(a)–3(e). Clearly, with increasing n, the corresponding PEMD shows increasingly better agreement with the reference result in Fig. 3(f), which is calculated by the split-operator spectral method. By using the differential approach (as used in Fig. 2(b)) to compare these two treatments, we confirm that for $n = 30$, the approximate result is almost identical to the reference result. It demonstrates that the approximation method is accurate and computationally efficient.

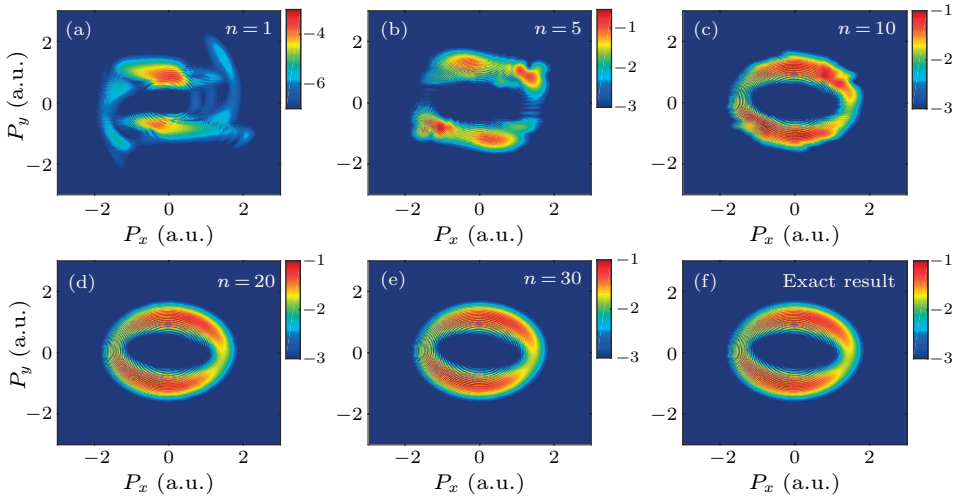


Fig. 3. PEMDs of Ar atoms induced by the circularly polarized laser pulse. (a) Simulated by the approximation method with the one-dimensional wavefunctions number $n = 1$, (b) $n = 5$, (c) $n = 10$, (d) $n = 20$, (e) $n = 30$. (f) Calculated result with the split-operator spectral method. The color scale is logarithmic.

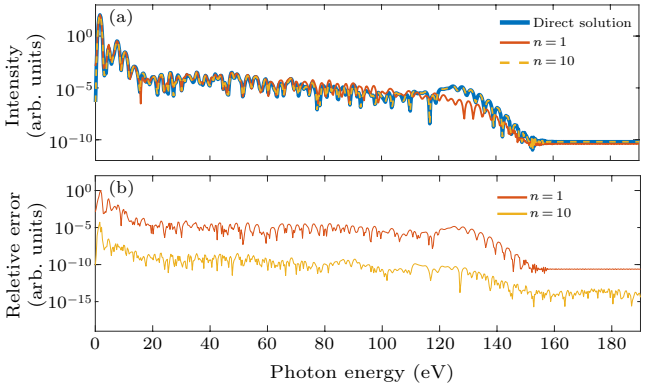


Fig. 4. (a) The high-order harmonic spectrum from H_2^+ molecular ion, using the approximation method with $n = 1$ (the red solid curve) and $n = 10$ (the yellow dashed curve), and the direct solution of the TDSE (the blue solid curve). (b) Relative error between the direct solution and the approximation method with $n = 1$ (the red curve) and $n = 10$ (the yellow curve).

In the above discussion, we calculate the PEMD of the tunneling ionization of the Ar atom. Both the split-operator spectral method and the approximation method are used to numerically solve the 2D TDSE and to obtain the real-time propagation of the electron wavefunction. The "ionized part" of the electron wavefunction is separated from the total time-dependent electron wavefunction and transformed into momentum space at the end of each time step to simulate the PEMD, and thus sizable computational demanding is required. In the subsequent discussion, we investigate the HHG of 1D non-Born–Oppenheimer hydrogen molecular ion subject to the linearly polarized laser pulse given by Eq. (15). Here, we treat both the 1D electron and the 1D nuclear motion as two distinguishable quasi-particles. Similarly to calculating the PEMD, we numerically solve this 2D-TDSE and trace the temporal evolution of the electron wavefunction, where our approximation method can efficiently reduce the computational cost. Then the HHG spectrum is calculated as the modulus squared of the Fourier transform of the dipole acceleration $a(t) = \mathrm{d}^2\langle\psi(t)|z|\psi(t)\rangle/\mathrm{d}t^2$, which is computational less demanding compared to simulating PEMD.

Figure 4(a) presents the HHG spectra from the H_2^+ molecular ion simulated by the approximated method and the direct method (solving TDSE directly), and Fig. 4(b) presents the relative error between these two methods. For the approximation method, the result shows an improvement with increasing number n of the one-dimensional wavefunctions. When $n = 10$, the spectrum displays remarkable agreement with the direct solution. Note that Figs. 1(c) and 3(c) demonstrate that, for $n = 10$, the approximation method is not accurate enough. This indicates that calculating PEMD requires more 1D wavefunctions to simulate the temporal evoluting electron wavefunction in Eq. (6).

4. Conclusion

In summary, we have demonstrated an approximation method to solve the 2D TDSE and utilize this method for exactly solvable systems. In this approach, the 2D electron wavefunction is expanded in terms of the multiplication of two serials of 1D wavefunctions. The equation of motion for the expansion coefficients and 1D wavefunctions are derived. Employing this approximation method to the investigation of the atom and molecule irradiated by the intense laser field, the PEMD and high-harmonic spectrum can be accurately and computationally simulated efficiently. Moreover, this framework is highly flexible, and thus it would enable more efficient simulations of the laser–matter interaction. For example, it can be straightforwardly extended to solve real three-dimensional TDSE for atoms and molecules in intense laser fields. By writing the three-dimensional wavefunction in Cartesian coordinates as $\psi(x,y,z)$, analogously to Eq. (6), we can write the wavefunction as a linear combination of lower-dimensional wave function products $\psi(x,y,z) = \sum_{ij}^{n} c_{ij}(t)\chi_i(x,y,t)\phi_j(z,t)$.

The derived equations of motion can be directly applied. Note that in this case, separation of the wavefunction into three quasi-particles according to three directions is not recommend, because in this case the coulomb potential would be a three-particle interaction term and will highly complicate the equations of motion. Moreover, our approximation method can use OpenMP with shared memory for parallel computing, and it is more difficult to imply MPI computing with distributed memory than directly solve the time-dependent Schrödinger equation.

Acknowledgments

Project supported by the National Natural Science Foundation of China (Grant Nos. 12204545 and 12274294) and the Program for NUE independent research and development.

References

[1] Agostini P and DiMauro L F 2004 *Rep. Prog. Phys.* **67** 1563
[2] Li J, Ren X, Yin Y, *et al.* 2017 *Nat. Commun.* **8** 186
[3] Hu F, Zhang Q, Cao J, Hong Z, Cao W and Lu P 2022 *Opt. Lett.* **47** 389
[4] Becker W, Grasbon F, Kopold R, Milošević D B, Paulus G G and Walther H 2002 *Adv. At. Mol. Phys.* **48** 35
[5] He M, Zhou Y, Li Y, Li M, Cao W and Lu P 2018 *Phys. Rev. Lett.* **120** 133204
[6] Zhao Y, Zhou Y, Liang J, Ke Q, Liao Y, Li M and Lu P 2022 *Phys. Rev. A* **106** 063103
[7] Corkum P 1993 *Phys. Rev. Lett.* **71** 1994
[8] Li L, Lan P, He L, Zhu X, Chen J and Lu P 2018 *Phys. Rev. Lett.* **120** 223203
[9] Li Y, Sato T and Ishikawa K 2019 *Phys. Rev. A* **99** 043401
[10] Xia C, Li Z, Liu J, Zeng A, Lü L and Bian X 2022 *Phys. Rev. A* **105** 013115
[11] He L, Sun S, Lan P, He Y, Wang B, Wang P, Zhu X, Li L, Cao W, Lu P and Lin C D 2022 *Nat. Commun.* **13** 4595
[12] Krausz F and Ivanov M 2009 *Rev. Mod. Phys.* **81** 163
[13] Gallmann L, Cirelli C and Keller U 2012 *Annu. Rev. Phys. Chem.* **63** 447
[14] Bauer D and Koval P 2006 *Comput. Phys. Commun.* **174** 396
[15] Tulsky V and Bauer D 2020 *Comput. Phys. Commun.* **251** 107098
[16] Morales F, Bredtmann T and Patchkovskii S 2016 *J. Phys. B: At. Mol. Opt. Phys.* **49** 245001
[17] He P, Lao D and He F 2017 *Phys. Rev. Lett.* **118** 163203
[18] Ishikawa K and Sato T 2015 *IEEE J. Sel. Top. Quantum Electron* **21** 8700916
[19] Li Y, Sato T and Ishikawa K 2021 *Phys. Rev. A* **104** 043104
[20] Kohn W and Sham L J 1965 *Phys. Rev.* **140** A1133
[21] Zanghellini J, Kitzler M, Fabian C, Brabec T and Scrinzi A 2003 *Laser Phys.* **13** 1064
[22] Nest M, Klamroth T and Saalfrank P 2005 *J. Chem. Phys.* **122** 124102
[23] Sato T, Ishikawa K L, Březinová I, Lackner F, Nagele S and Burgdörfer J 2016 *Phys. Rev. A* **94** 023405
[24] Kato T and Kono H 2004 *Chem. Phys. Lett.* **392** 533
[25] Protopapas M, Keitel C H and Knight P L 1997 *Rep. Prog. Phys.* **60** 389
[26] Tong X M, Hino K and Toshima N 2006 *Phys. Rev. A* **74** 031405
[27] Chelkowski S, Foisy C and Bandrauk A 1998 *Phys. Rev. A* **57** 1176
[28] Keldysh L 1998 *Sov. Phys. JETP* **20** 1307
[29] Feit M D, Fleck Jr. J A and Steiger A 1982 *J. Comput. Phys.* **47** 412
[30] Huismans Y, Rouzée A, Gijsbertsen A, Jungmann J, Smolkowska A, Logman P, Lépine F, Cauchy C, Zamith S, Marchenko T, Bakker J, Berden G, Redlich B, van der Meer A, Muller H, Vermin W, Schafer K, Spanner M, Ivanov M, Smirnova O, Bauer D, Popruzhenko S and Vrakking M 2011 *Science* **331** 61
[31] He M, Fan Y, Zhou Y and Lu P 2021 *Chin. Phys. B* **30** 123202
[32] Zhou Y, Tolstikhin O I and Morishita T 2016 *Phys. Rev. Lett.* **116** 173001